Magnetic-Assisted Treatment of Liver Fibrosis

Subjects: Gastroenterology & Hepatology | Biochemistry & Molecular Biology

Contributor: Ralf Weiskirchen

Chronic liver injury can be induced by viruses, toxins, cellular activation, and metabolic dysregulation and can lead to liver fibrosis. Hepatic fibrosis still remains a major burden on the global health systems. Nonalcoholic fatty liver disease (NAFLD) and nonalcoholic steatohepatitis (NASH) are considered the main cause of liver fibrosis. Hepatic stellate cells are key targets in antifibrotic treatment, but selective engagement of these cells is an unresolved issue.

liver fibrosis immune cells

1. Methods for Synthesis of Magnetic Nanomedicines

The various types of synthesis strategies for MNP can be separated into two approaches: top-down and bottom-up. The “bottom-up approach” starts from metal ions in solution via chemical methods and is probably the most commonly used strategy. The top-down approach starts with bulk material, which is further processed, i.e., by laser ablation [1][2][3][4][5] or lithography [6][7][8][9] including that of nanospheres [9]. The lithography techniques have broad control on the shape of nano or microstructures; however, the scaling of this method to large-scale production was reported to be challenging [10]. The laser ablation method offers the building of quite complicated structures such as core-shell MNPs and has a lot of degrees of freedom for adjustment by variation of the environment, material of target, laser regime, as well as external stimulus, for example, magnetic or electrical field to change the shape and structural properties of MNPs [1][4]. This method beats some drawbacks of more common chemical methods; for example, it does not require high temperature, pressure, or organometallic precursors to obtain MNPs with excellent magnetic properties [5][11]. Thus, the laser ablation method has great potential to set higher standards in nanoparticle production.

However, many methods are combinations of both types of methods. For example, the known ball milling method of the MNP preparation is popular for permanent magnet fabrication [12]. It allows one to scale up the synthesis to an industrial scale, although the control of particle shape and size is difficult. Potential agglomerations of nanoparticles can occur which makes the particles unsuitable for biomedical applications [12]. Nevertheless, in combination with chemistry, the ball milling equipment can be used in the so-called mechanochemical process. Here, for instance, a nanocomposite of MNPs in the benzene-1,3,5-tricarboxylic acid matrix was obtained via a mechanochemical process [13]. The obtained material was porous and defined as a metal-organic framework. This nanocomposite was tested for a drug delivery application to release doxorubicin as a model drug. The authors noted that the high surface area of such porous materials favors an increased loading rate, while the magnetic properties of this material offer novel perspectives for diagnostic systems [13].

Typical synthesis steps of chemical methods consist of different steps, particularly burst nucleation, and the following nanocrystal grow, which is called Ostwald ripening [14][15]. Control of reaction kinetics by varying temperature, solvent or other conditions, and operation with the Ostwald process by pH control and electrostatic repulsion of nuclei allow us to systematically vary the size of the particles [15]. It is of utmost importance to obtain nanoparticles with precise and predefined size, shape, and phase composition [16][17]. It was suggested to evaluate the most commonly used synthesis strategies by the four-word strengths, weaknesses, opportunities, and threats (SWOT) analysis for applications in molecular recognition [17]. The research group evaluated the co-precipitation, thermal decomposition (HTD), microemulsion, and microfluidic synthesis method and studied dual-particles consisting of several materials. The first one, co-precipitation, is an easy to use technique to obtain large amounts of MNPs by alkalization of metal salt solutions. First demonstrated in 1981 by Massart, this method is beneficial and allows us to produce well-crystallized iron oxide or ferrite MNPs in the size range of 10−30 nm [18][19][20]. The drawbacks of this method are the poor control of shape and size distribution; moreover, for smaller particles, less than 10 nm, the quality of crystals decreases and the number of disordered spins leads to a change in the magnetic properties [21]. Advanced co-precipitation methods are performed at high temperature and pressure, by hydrothermal surface treatment, or hydrothermal routes [22][23][24], as well as in non-aqueous medium by solvothermal methods [25][26][27]. The polyol process is another interesting method which is a cost-effective and easily scalable method to produce MNPs of high quality and variety morphology, from simple pseudo-spherical to multi-core nanoflowers of core-shell MNPs [28][29][30]. In the polyol process, solvents also play the role of a reducing agent and a surfactant.

Invented in 2004 for the synthesis of MNPs, the HTD method allows us to obtain MNPs with a narrow size distribution and high crystallinity [31][32][33]. MNPs produced with this method have a high value of magnetization, favoring their use in many biological applications, including sensors and detection [21][34]. According to the SWOT analysis above described [17], a drawback of this method is that it is time consuming and expensive. Precise shape control can be achieved by varying the experimental conditions. For instance, a variation of ligands and surfactants offers advantages for both magnetic properties and the related behavior in biological environments [16][35][36]. The group of Jinwoo Cheon [37][37] demonstrated higher magnetization values of cubic MNPs (165 emu/g_{Fe+Zn}) compared to spherical (145 emu/g_{Fe+Zn}) particles. The difference can be attributed to the lower amount of disordered spins on the surface. It was also reported that cubic shaped MNPs on the sensor‘s surface exhibit a higher binding ability because of the higher contact area of planar interface compared to the spherical one [35]. Furthermore, cubic MNPs exhibited stronger signals, as evaluated by giant magnetoresistive sensing (GMR) and force-induced remnant magnetization spectroscopy (FIRMS).

There are various methods for co-precipitation with different modifications, which, together with HTD, are the most frequently used methods for MNP synthesis [17]. Co-precipitation represents the most important production method: it is easy, cheap, and enables a rapid synthesis. The generated particles have hydrophilic surfaces, which can be functionalized in situ. The second most important method, HTD, allows one to produce MNPs with well-defined shape and narrow size distribution. However, the low amount of reaction products, high-cost reagents, and hydrophobic surfaces, which can be functionalized in the multi-step process, make this method currently mostly interesting only for research activity.

2. Clinical Use and Further Perspectives Iron Oxide

Currently, Feraheme® (ferumoxytol) which is approved by the U.S. Food and Drug Administration (FDA) as well as in Europe and Canada is the most successful iron oxide-based drug. It is prescribed to patients with iron deficiency anemia and chronic kidney disease. It can be considered as a great advantage that iron is a naturally occurring element of the body which also leaves the body via natural pathways of iron metabolism [38]. Feraheme is based on non-stoichiometric magnetite MNPs with diameter (d) ~ 7 nm and hydrodynamic diameter (d_H) = 28–33 nm coated with carboxy-dextran. Feraheme is also an 'off label' magnetic resonance angiography (MRA) and magnetic resonance imaging (MRI) contrast agent [39]. In order to study MNP uptake by macrophages in vivo, high-resolution 3D-maps of pancreatic inflammation were generated using MRI and it showed that the MNP uptake by macrophages was higher in the inflamed pancreatic lesion in T1D-models [40]. Therefore, the special properties of the inflammatory setting on noninvasive imaging have to be considered. The capability of iron oxide to produce reactive oxygen species (ROS) was recently discovered to be usable in order to treat leukaemia [41]. In contrast to intravenously administrated drugs, the oral delivery (OD) is more popular with patients. Yet, the passage of the gastrointestinal (GI) tract, which has a very low pH level, [42] is a problem for iron oxides since they degrade at this pH. Thus, to overcome this limitation, a coating is required which is stable in the wide pH range of 2–8. Coatings such as gold or silica oxide are applicable for this purpose since these materials are stable in the GI tract.

Mesenchymal stem cells (MSC) have been demonstrated to be a promising tool for the treatment of many types of human diseases, including liver fibrosis and hepatocellular carcinoma (HCC) [43][44][45][46][47]. Labeling of MCS with MNPs can be used as a supplementary diagnostic approach. Recently, Faidah at al., proved that application of MNPs have not changed the viability and proliferative capabilities of MSCs in a rat cirrhosis model based on a carbon tetrachloride (CCl_4) model for toxic liver injury [48]. Additionally, similar results by Lai and co-authors have shown that MSCs that overexpress human hepatocyte growth factor (HGF) promote liver recovery in a rat liver fibrosis model [49]. Further, labeling of MSC with NP led to an accumulation of the cells in MRI-based imaging [48][49], which seems to confirm the idea that magnetic NPs in liver fibrosis can be used as a diagnostic agent for MRI.

The off-label use of feraheme is continuing to grow. The assessment of the stage of liver fibrosis remains a key issue in patient diagnostics. Currently, the gold standard is still given by a liver biopsy while imaging techniques as elastography and relaxometry have not been elaborated in this regard, particularly, for proving moderate fibrosis [50]. A recent study showed that patients with different stages of liver fibrosis exhibited MRI-assessible differences. One should, however, be aware that T2 parameters can be quantified via a dual echo turbo-spin echo technique. Besides, these applications can also help to understand different stages of fibrosis patients [51]. It is noticeable that T2 or negative contrast agents possess superparamagnetic properties and are represented by nanoparticles with iron oxide core or other magnetic materials [51]. For this purpose, researchers are using different types of synthesis, shapes and covering of nanoparticles with magnetic cores. One should, nevertheless, consider the associated problems from another perspective: Li and coworkers proposed to conjugate Fe_3O_4 NPs with immunofluorescence markers (indocyanine green (ICG). Further, a targeting ligand for integrin avb3, arginine–glycine–aspartic acid (RGD) expressed by HSCs to detect early stages of liver fibrosis, was used [52]. A similar approach was used by Zhang and coauthors, who investigated diagnostic of liver fibrosis stages in a rat model induced by CCl_4 injection.

Although they were using molecular MRI with RGD peptide, modified ultrasmall superparamagnetic iron oxide nanoparticles (USPIO) were demonstrated to be a promising tool for noninvasive imaging of the progression of the liver fibrosis [53].

Furthermore, one should note that together with the advantageous properties of magnetic materials which makes them usable as MRI contrast agents, the iron overload in tissues can be really harmful. Thus, Wei and coauthors reported that a single dose of MNP application at a high concentration (5 mg Fe/kg) induced a septic shock response at 24 h and provoked high levels of serum markers (ALT, AST, cholesterol and other markers), which was noted within 14 days. Moreover, a high dose of MNPs activated significant expression changes of a distinct subset of genes in cirrhosis liver compared with a normal dose of MNP application (0.5 mg Fe/kg) [54]. Furthermore, Lunov et. al. analyzed the impact of MNPs on macrophages and demonstrated that overload of iron leads to apoptosis in these cells, which is mediated via activation of the c-Jun N-terminal kinase (JNK) pathway [55]. This investigation demonstrated that iron overload caused by MNP application may have dramatic effects, particularly on the liver, which contains a large numbers of macrophages.

3. Magnetic Hybrid Nanomaterials

Iron oxides exhibit moderate cytotoxicity; however, for their use in biomedicine, such aspects as biotransformation, biodistribution and in-blood circulating time should be controlled [56]. Because of this reason, the iron oxide MNPs can be hybridized, i.e., with certain polymers (dextran, chitosan, PEG) [57], noble metals (Au, Ag) [58][59], non-magnetic oxides (MgO, ZnO) [60][61], or silica dioxide (SiO_2) [62]. Apart from polysaccharides, PEG is more often used for organic coating of MNPs. By varying the molecular weight of the PEG from 6000 to 50,000, it is possible to prolong the circulation time (blood half-life) from 30 min to one day [63]. The coating leads to a change in the surface charge of MNPs and, therefore, also significantly affects the pharmacokinetic behavior. Typically, the negatively charged MNPs exhibit a longer blood half-life. The coating also makes it easier to modify the surface for modifications with biomolecules, genes, or drugs. Furthermore, hybrid materials possess additional functionalities, for instance, nano-dimensional gold exhibits the surface plasmon resonance phenomenon changing the optical properties of the material, which can be exploited for the detection in photothermal therapy [58][64][65]. Maria Efremova and her colleagues reported on nanohybrids of magnetite and gold in the form of Janus-like MNPs [58]. Two district surfaces established a platform for conjugation with two different molecules, for example, with fluorescent dyes or drugs. These nanohybrids exhibited enhanced contrast for MRI and allowed tracking delivery of the attached drug in a real-time fashion via intravital fluorescent microscopy.

Lipid-based nanomedicines represent the nanomedicines with the highest market value. Via a combination of SPIONs embedded into the lipid membrane of liposomes, the desired properties of both materials can be combined. One example of an application with magnetoliposomes is the application of a magnetic field to induce release of nucleic acids, such as DNA, which might be useful in drug release. Salvatore et al. demonstrated that SPIONs can trigger release of DNA from a multifunctional hybrid nanomaterial composed of liposome components, double-stranded DNA, and hydrophobic SPIONs [66].

Their numbers are very likely to further increase in future nanomedicines.

4. Magnetic-Assisted Medical Applications

The size of nanomaterials is a critical factor for their behavior and distribution in the body. Small particles in the blood tend to aggregate or to be decorated with a protein corona and, because of their charge, create an electrical double layer. In this sense, the total size of particles characterized by the hydrodynamic diameter (d_H) can be measured i.e., using dynamic light scattering (DLS) [67]. Both the hydrodynamic and physical size of MNPs determine their magnetic properties. In circulation, systemically injected MNPs circulate in the lumen of blood vessels, interacting with macrophages of the reticuloendothelial system (RES). Smaller USPIONs with d_H > 10 nm were characterized by longer blood half-life than SPIONs d_H > 50 nm [63]. Depending on the hydrodynamic size as well as the electrical charge and other properties, pharmacokinetics and biodistribution of MNPs are rendered [68]. MNPs with a d_H below than 15 nm are filtered by the kidney; MNPs with a d_H less than 100 nm accumulate in the liver in hepatocytes and Disse space; a d_H of 100–150 nm leads to the primary accumulation in liver that is based on the uptake by Kupffer cells and these larger hydrodynamic particles can also be trapped by splenic macrophages.

Since the liver and spleen are primary targets for MPN accumulation, they can also be targeted with these particles. The hydrodynamic size of 10–50 nm seems optimal for longer circulation time, but it should be stressed that not only size matters, but properties of the surface such as zeta-potential and hydrophilic/hydrophobic properties are critical factors for biodistribution [63]. Non-specific biodistribution of MNPs was used for MRI enhancement of liver disease [68][69]. Ferrucci and Starkre reported that 80% of intravenously injected non-specific SPIONs were internalized by Kupffer cells. Thereby, the MNPs create an MR-contrast that enables us to trace hepatic neoplasms [69].

Four non-exhaustive areas in which magnetic materials are important (**Table 1**). The first area includes the biggest success story for using magnetic fields for binding-mediated cell capturing. The chimeric antigen receptor (CAR) T cells have significantly advanced tumor therapies. This technology is based on the isolation of T cells from autologous donors and these cells are genetically engineered to target a specific antigen. The isolation of T cells is currently approved for treatment of B cell lymphoma, and it is expected that T cell engineering will enrich many other fields as well; clinical studies are ongoing in liver cancer. The group of Michael Sadelain pioneered T cell engineering and they have recently shown that macrophages play a key role in mediating the side effects of CAR T cell therapy [70]. Other groups also attempt to manipulate other immune cells, such as natural killer cells [71]. Microfluidics that facilitate binding-mediated cell capturing and release is a key technology for sorting cells in closed systems [72][73][74]. The microfluidic concept for manufacturing lab-on-a-chip devices use MNPs and these allow for a quick analysis and an automated composition of an individual treatment. Currently, the CAR T cell therapies are mainly focused on B cell malignancies, but other types of cancer are being explored in clinical trials.

Table 1. Selected areas of applications for magnetic nanoparticles.

Role of MNP[1]	Area of Biomedical Application	Literature
Binding-mediated cell capturing	Cell isolation and separation	[70][72][73][74]
	Cell and tissue engineering	[75][76][77]
	Cell patterning and concentration	[78][79][80][81][82]
Mechanical cell control	Low-frequency magnetic field for cell destruction and induction of apoptosis	[7][84][85]
	Differentiation of stem cells, modulation of cell division and motility	[86][87][88]
	Fundamental study of macromolecules and cell's mechanical properties	[89][90]
Drug delivery	Magnetic fluid hyperthermia of cancer	[64][91][92]
	On-demand release of drugs via thermosensitive polymers or azo molecules from hybrid nanoplatforms	[62][93][94]
	Targeting or delivery of drug or genes immobilized on surfaces	[95][96][97][98]
Imaging applications	Reduction of T_1 and T_2 relaxation time of the water protons for the MRI-contrast	[53][99]
	Imaging and detection via a non-linear magnetic signal	[101][102]
	Improved detection of magnetic signals, imaging of liver fibrosis	[103][104]

[1] MNP: Magnetic nanoparticle(s).

Tissue engineering has been given further opportunities by magnetic fields, i.e., by facilitating the arrangement of different cellular layers [75][76][77]. Magnetic fields have been used to establish three-dimenstional cell culture arrays, to enable cell patterning for the evaluation of the effect of fibroblasts on their capability of infiltration [78][79][80]. Rieck et al. recently demonstrated that magnetic nanocarriers can be localized in specific areas of the body using magnetic fields. Their approach was done using complexes of lentivirus and MNPs in combination with magnetic fields. The group highlighted that using this method in the murine embryonic stem cell system offers the opportunity to site-specifically downregulate protein tyrosine phosphatase SHP2 by RNAi technology in selected areas with the pathogenic vessel formation [81]. Using this principle would allow us to selectively transmit a specific payload to immune cells based on phagocytic uptake to diseased sites in the liver. Muthana et al. demonstrated that even magnetic resonance imaging machines might be usable to control the spatial concentration of MNPs [82].

Here, the aim is to get control over the mechanical properties of cells. In the near future, the technology may be used to measure the stiffness of biological molecules or cellular organelles in vivo. Magnetic tweezers are used as a simple tool to study mechanical forces of biological molecules and cells [83]. Low-frequency magnetic fields are applicable for directed cell destruction and induction of apoptosis [7][84][85]. The concept of mechanical cell control has already been used to function as a cellular remote control, to modulate the stem cells differentiation, or to modulate the behavior of single cells [86][87][88]. Magnetic micromanipulation based on the application of magnetic

tweezers is a potent biophysical technique that is applicable for single-molecule unfolding, rheology measurements, and analyses of force-regulated processes in living cells [89][90].

The third type of application is drug delivery. MNPs are a powerful tool for therapy to target killing of injured or infected cells, which may be achieved by, for example, native toxicity of the MNPs, thermomagnetic effect in magnetic hyperthermia, or targeted drug delivery and release [64][91][92]. In particular, the field of drug delivery can potentially be highly enriched by magnetism-based applications. In addition to the above-mentioned application of MRI scanners to spatially concentrate magnetic particles, magnetic fluids, meaning magnetic particles in a dispersion, might be controlled magnetically. The release of drugs, for example, mediated by magnetism-enhanced thermosensitive polymers, might also be enriched by magnetic actions, for example, to trigger the release of different drugs from a single carrier from porous materials, remote-controlled drug release using azo-functionalized iron oxide nanoparticles, or in order to trigger heat and drug release from magnetically controlled nanocarriers [62][93][94]. In addition to particulate or crystal-based systems, surface immobilized iron might be controlled using noninvasive magnetic stimulation [95][96][97][98].

The fourth area in which magnetism has been used intensively is applications based on imaging. For instance, MRI-based imaging of liver fibrosis can be enabled by visualizing fibrosis based on non-invasive analysis of collagen or elastin. Fibrosis might even be visualized by labeling HSC, i.e., by monitoring a specific surface marker such as the folate-receptor, that has already been used for this purpose. Folate receptor-targeted particles have also led to improved specificity of tissue binding [53][99]. In order to enable an early therapy of fibrosis, it is critical that it is also diagnosed at early stages. However, there is currently no established early stage marker. In the future, improved early recognition techniques such as circulating collagen fragments, i.e., the N-terminal propeptide of collagen III (Pro-C3) will very likely enable to perform “liquid biopsies” for early detection of fibrosis. Screening of Pro-C3 in plasma of patients has already been done in hepatitis C patients and has been demonstrated to be able to predict fibrosis progression [99]. Other biomarkers might be circulating micro-RNA, and other types of RNA, such as long non-coding RNA (LncRNA), epigenetic analyses, and microbiome studies. Usually, biomarkers work best if they are combined to calculate a specific score such as the NAFLD fibrosis score, the fibrosis 4 (FIB-4) index, or the aspartate aminotransferase to platelet ratio index (APRI) score.

Non-invasive imaging techniques have high potential to confirm the findings from biomarker screening. Consequently, there is a high unmet need for the development of improved techniques for non-invasive diagnosis of liver fibrosis [45]. In ref. [45], the molecular MRI was used for distinguishing different fibrosis stages in a CCl_4-based rat model. Enhanced accuracy of [53]detection was achieved by using a targeted USPIO-based contrast agent for MRI. The MRI contrast depends on the time of relaxation of protons that alters in the presence of a magnetic field generated by MNPs and it depends on the degree of interaction of the MNPs with protons. Furthermore, direct imaging of the distribution of MNPs is possible by magnetic particle imaging (MPI) introduced in 2005 and based on measurements of the nonlinear magnetic signal of MNPs [101][102]. Potentially, MPI can enable an improved spatial and temporal resolution than the resolution of the MRI and because of the native biodistribution of iron oxide-based MNPs, the use of this technique for liver seems promising. Improved detection methodologies may also further improve the usage of magnetic particles as biosensors [103]. Imaging probes such

as those monitoring Elastin will very likely also improve imaging of liver fibrosis at later stages of the disease, as Elastin appears in late-stage fibrosis [104].

The tripeptide arginine-glycine-aspartic acid (RGD) binds to integrin αvβ3 expressed on HSCs [53]. Conjugation with RGD significantly improved targeting of administrated USPIONs [53]. This allowed the authors to differentiate various liver fibrosis stages with MRI. The relaxivity of developed nanoparticles was higher than, for example, the earlier reported collagen-specific contrast agent based on Gd^{3+}. Further improvement was done by multimodal imaging with nanohybrids [52]. In this study, it was suggested that the conjugation of USPIONs-SiO_2 with indocyanine green (ICG) dye may further improve near-infrared fluorescence imaging and RGD for targeting. This combination of imaging modalities enables it to perform multimodal imaging (NIR and MRI). To establish theranostic platforms, an additional drug should be attached [105][106].

In particular, cell sorting technology which is currently enabling breakthroughs in cancer therapy is largely based on magnetic forces to sort cells, i.e., the magnetic-assisted cell sorting technology (MACS). These technologies are based on magnetic fields and enable sorting and manipulate cells in closed systems. Mechanical cell control is still in its infancy, but may significantly enrich single cell analysis methods. The field of drug delivery may assumingly expect high potential for breakthroughs due to the potential localized targeting of tissues or cells in vivo, to reduce side effects on non-target cells with enhanced specificity. Imaging applications are already profiting from steadily improved probes, improved methods for signal detection, and better biological targets. In fibrosis imaging, non-invasive assessment of Collagen and Elastin might in future enable significantly improved and more specific assessment of liver fibrosis (**Figure 1**).

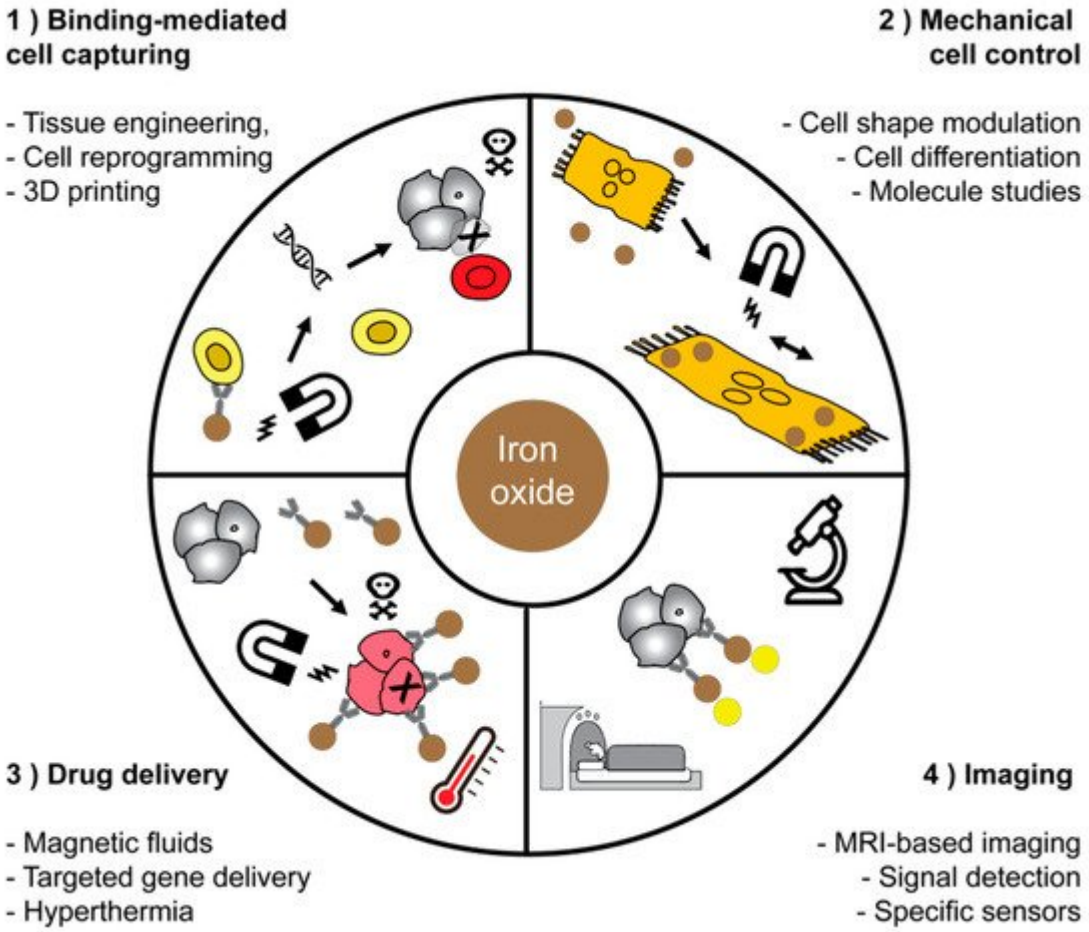

Figure 1. Applications of magnetic nanoparticles in medicine and biotechnology. Four main fields of application for magnetic materials were highlighted and have chosen some representative schemes for each field of application.

References

1. Wagener, P.; Jakobi, J.; Rehbock, C.; Chakravadhanula, V.S.K.; Thede, C.; Wiedwald, U.; Bartsch, M.; Kienle, L.; Barcikowski, S. Solvent-surface interactions control the phase structure in laser-generated iron-gold core-shell nanoparticles. Sci. Rep. 2016, 6, 23352.
2. Maneeratanasarn, P.; Khai, T.V.; Kim, S.Y.; Choi, B.G.; Shim, K.B. Synthesis of phase-controlled iron oxide nanoparticles by pulsed laser ablation in different liquid media. Phys. Status Solidi A 2013, 210, 563–569.
3. Fazio, E.; Santoro, M.; Lentini, G.; Franco, D.; Guglielmino, S.P.P.; Neri, F. Iron oxide nanoparticles prepared by laser ablation: Synthesis, structural properties and antimicrobial activity. Colloids Surf. A 2016, 490, 98–103.
4. Xiao, J.; Liu, P.; Wang, C.; Yang, G. External field-assisted laser ablation in liquid: An efficient strategy for nanocrystal synthesis and nanostructure assembly. Prog. Mater. Sci. 2017, 87, 140–220.

5. Amendola, V.; Meneghetti, M.; Granozzi, G.; Agnoli, S.; Polizzi, S.; Riello, P.; Boscaini, A.; Anselmi, C.; Fracasso, G.; Colombatti, M. Top-down synthesis of multifunctional iron oxide nanoparticles for macrophage labelling and manipulation. J. Mater. Chem. 2011, 21, 3803–3813.
6. Vitol, E.A.; Novosad, V.; Rozhkova, E.A. Microfabricated magnetic structures for future medicine: From sensors to cell actuators. Nanomedicine 2012, 7, 1611–1624.
7. Kim, D.-H.; Rozhkova, E.A.; Ulasov, I.V.; Bader, S.D.; Rajh, T.; Lesniak, M.S.; Novosad, V. Biofunctionalized magnetic-vortex microdiscs for targeted cancer-cell destruction. Nat. Mater. 2010, 9, 165.
8. Litvinov, J.; Nasrullah, A.; Sherlock, T.; Wang, Y.-J.; Ruchhoeft, P.; Willson, R.C. High-throughput top-down fabrication of uniform magnetic particles. PLoS ONE 2012, 7, e37440.
9. Kosiorek, A.; Kandulski, W.; Glaczynska, H.; Giersig, M. Fabrication of nanoscale rings, dots, and rods by combining shadow nanosphere lithography and annealed polystyrene nanosphere masks. Small 2005, 1, 439–444.
10. del Campo, A.; Arzt, E. Fabrication approaches for generating complex micro-and nanopatterns on polymeric surfaces. Chem. Rev. 2008, 108, 911–945.
11. Svetlichnyi, V.; Shabalina, A.; Lapin, I.; Goncharova, D.; Velikanov, D.; Sokolov, A. Characterization and magnetic properties study for magnetite nanoparticles obtained by pulsed laser ablation in water. Appl. Phys. A 2017, 123, 763.
12. Yue, M.; Zhang, X.; Liu, J.P. Fabrication of bulk nanostructured permanent magnets with high energy density: Challenges and approaches. Nanoscale 2017, 9, 3674–3697.
13. Bellusci, M.; Guglielmi, P.; Masi, A.; Padella, F.; Singh, G.; Yaacoub, N.; Peddis, D.; Secci, D. Magnetic Metal–Organic Framework Composite by Fast and Facile Mechanochemical Process. Inorg. Chem. 2018, 57, 1806–1814.
14. Thanh, N.T.; Maclean, N.; Mahiddine, S. Mechanisms of nucleation and growth of nanoparticles in solution. Chem. Rev. 2014, 114, 7610–7630.
15. Vayssieres, L.; Chanéac, C.; Tronc, E.; Jolivet, J.P. Size tailoring of magnetite particles formed by aqueous precipitation: An example of thermodynamic stability of nanometric oxide particles. J. Colloid Interface Sci. 1998, 205, 205–212.
16. Roca, A.G.; Gutierrez, L.; Gavilán, H.; Brollo, M.E.F.; Veintemillas-Verdaguer, S.; del Puerto Morales, M. Design strategies for shape-controlled magnetic iron oxide nanoparticles. Adv. Drug Deliv. Rev. 2018, 138, 68–104.
17. Salvador, M.; Moyano, A.; Martínez-García, J.C.; Blanco-López, M.C.; Rivas, M. Synthesis of Superparamagnetic Iron Oxide Nanoparticles: SWOT Analysis Towards Their Conjugation to

Biomolecules for Molecular Recognition Applications. J. Nanosci. Nanotechnol. 2019, 19, 4839–4856.

18. Massart, R. Preparation of aqueous magnetic liquids in alkaline and acidic media. IEEE Trans. Magn. 1981, 17, 1247–1248.
19. Daffé, N.; Choueikani, F.; Neveu, S.; Arrio, M.-A.; Juhin, A.; Ohresser, P.; Dupuis, V.; Sainctavit, P. Magnetic anisotropies and cationic distribution in CoFe2O4 nanoparticles prepared by co-precipitation route: Influence of particle size and stoichiometry. J. Magn. Magn. Mater. 2018, 460, 243–252.
20. Yelenich, O.; Solopan, S.; Kolodiazhnyi, T.; Tykhonenko, Y.; Tovstolytkin, A.; Belous, A. Magnetic properties and AC losses in AFe2O4 (A= Mn, Co, Ni, Zn) nanoparticles synthesized from nonaqueous solution. J. Chem. 2015, 2015, 532198.
21. Nedelkoski, Z.; Kepaptsoglou, D.; Lari, L.; Wen, T.; Booth, R.A.; Oberdick, S.D.; Galindo, P.L.; Ramasse, Q.M.; Evans, R.F.; Majetich, S. Origin of reduced magnetization and domain formation in small magnetite nanoparticles. Sci. Rep. 2017, 7, 45997.
22. Jovanovic´, S.; Spreitzer, M.; Otonic˘ar, M.; Jeon, J.-H.; Suvorov, D. pH control of magnetic properties in precipitation-hydrothermal-derived CoFe2O4. J. Alloys Compd. 2014, 589, 271–277.
23. Gomes, J.d.A.; Sousa, M.H.; Tourinho, F.A.; Aquino, R.; da Silva, G.J.; Depeyrot, J.; Dubois, E.; Perzynski, R. Synthesis of core− shell ferrite nanoparticles for ferrofluids: Chemical and magnetic analysis. J. Phys. Chem. C 2008, 112, 6220–6227.
24. Pilati, V.; Cabreira Gomes, R.; Gomide, G.; Coppola, P.; Silva, F.G.; Paula, F.b.L.; Perzynski, R.G.; Goya, G.F.; Aquino, R.; Depeyrot, J. Core/shell nanoparticles of non-stoichiometric Zn–Mn and Zn–Co ferrites as thermosensitive heat sources for magnetic fluid hyperthermia. J. Phys. Chem. C 2018, 122, 3028–3038.
25. Sanna Angotzi, M.; Musinu, A.; Mameli, V.; Ardu, A.; Cara, C.; Niznansky, D.; Xin, H.L.; Cannas, C. Spinel ferrite core–shell nanostructures by a versatile solvothermal seed-mediated growth approach and study of their nanointerfaces. ACS Nano 2017, 11, 7889–7900.
26. Liu, X.; Liu, J.; Zhang, S.; Nan, Z.; Shi, Q. Structural, magnetic, and thermodynamic evolutions of Zn-doped Fe3O4 nanoparticles synthesized using a one-step solvothermal method. J. Phys. Chem. C 2016, 120, 1328–1341.
27. Grabs, I.-M.; Bradtmöller, C.; Menzel, D.; Garnweitner, G. Formation mechanisms of iron oxide nanoparticles in different nonaqueous media. Cryst. Growth Des. 2012, 12, 1469–1475.
28. Muscas, G.; Yaacoub, N.; Concas, G.; Sayed, F.; Hassan, R.S.; Greneche, J.; Cannas, C.; Musinu, A.; Foglietti, V.; Casciardi, S. Evolution of the magnetic structure with chemical composition in spinel iron oxide nanoparticles. Nanoscale 2015, 7, 13576–13585.

29. Hemery, G.; Keyes, A.C., Jr.; Garaio, E.; Rodrigo, I.; Garcia, J.A.; Plazaola, F.; Garanger, E.; Sandre, O. Tuning sizes, morphologies, and magnetic properties of monocore versus multicore iron oxide nanoparticles through the controlled addition of water in the polyol synthesis. Inorg. Chem. 2017, 56, 8232–8243.
30. Franceschin, G.; Gaudisson, T.; Menguy, N.; Dodrill, B.C.; Yaacoub, N.; Grenèche, J.M.; Valenzuela, R.; Ammar, S. Exchange-Biased Fe3− xO4-CoO Granular Composites of Different Morphologies Prepared by Seed-Mediated Growth in Polyol: From Core–Shell to Multicore Embedded Structures. Part. Part. Syst. Charact. 2018, 35, 1800104.
31. William, W.Y.; Falkner, J.C.; Yavuz, C.T.; Colvin, V.L. Synthesis of monodisperse iron oxide nanocrystals by thermal decomposition of iron carboxylate salts. Chem. Commun. 2004, 2306–2307.
32. Sun, S.; Zeng, H.; Robinson, D.B.; Raoux, S.; Rice, P.M.; Wang, S.X.; Li, G. Monodisperse mfe2o4 (m= fe, co, mn) nanoparticles. J. Am. Chem. Soc. 2004, 126, 273–279.
33. Park, J.; An, K.; Hwang, Y.; Park, J.-G.; Noh, H.-J.; Kim, J.-Y.; Park, J.-H.; Hwang, N.-M.; Hyeon, T. Ultra-large-scale syntheses of monodisperse nanocrystals. Nat. Mater. 2004, 3, 891.
34. Kolhatkar, A.; Jamison, A.; Litvinov, D.; Willson, R.; Lee, T. Tuning the magnetic properties of nanoparticles. Int. J. Mol. Sci. 2013, 14, 15977–16009.
35. Yoo, D.; Lee, J.-H.; Shin, T.-H.; Cheon, J. Theranostic magnetic nanoparticles. Acc. Chem. Res. 2011, 44, 863–874.
36. Cotin, G.; Blanco-Andujar, C.; Nguyen, D.V.; Affolter-Zbaraszczuk, C.; Boutry, S.; Anne, B.; Ronot, P.; Uring, B.; Choquet, P.; Zorn, P.E. Dendron based antifouling, MRI and magnetic hyperthermia properties of different shaped iron oxide nanoparticles. Nanotechnology 2019, 30, 37.
37. Noh, S.-H.; Na, W.; Jang, J.-T.; Lee, J.-H.; Lee, E.J.; Moon, S.H.; Lim, Y.; Shin, J.-S.; Cheon, J. Nanoscale magnetism control via surface and exchange anisotropy for optimized ferrimagnetic hysteresis. Nano Lett. 2012, 12, 3716–3721.
38. Toth, G.B.; Varallyay, C.G.; Horvath, A.; Bashir, M.R.; Choyke, P.L.; Daldrup-Link, H.E.; Dosa, E.; Finn, J.P.; Gahramanov, S.; Harisinghani, M.; et al. Current and potential imaging applications of ferumoxytol for magnetic resonance imaging. Kidney Int. 2017, 92, 47–66.
39. Hood, M.N.; Blankholm, A.D.; Stolpen, A. The Rise of Off-Label Iron-Based Agents in Magnetic Resonance Imaging. J. Radiol. Nurs. 2019, 38, 38–41.
40. Gaglia, J.L.; Harisinghani, M.; Aganj, I.; Wojtkiewicz, G.R.; Hedgire, S.; Benoist, C.; Mathis, D.; Weissleder, R. Noninvasive mapping of pancreatic inflammation in recent-onset type-1 diabetes patients. Proc. Natl. Acad. Sci. USA 2015, 112, 2139–2144.

41. Trujillo-Alonso, V.; Pratt, E.C.; Zong, H.; Lara-Martinez, A.; Kaittanis, C.; Rabie, M.O.; Longo, V.; Becker, M.W.; Roboz, G.J.; Grimm, J. FDA-approved ferumoxytol displays anti-leukaemia efficacy against cells with low ferroportin levels. Nat. Nanotechnol. 2019, 14, 616.
42. Huang, J.; Shu, Q.; Wang, L.; Wu, H.; Wang, A.Y.; Mao, H. Layer-by-layer assembled milk protein coated magnetic nanoparticle enabled oral drug delivery with high stability in stomach and enzyme-responsive release in small intestine. Biomaterials 2015, 39, 105–113.
43. Shah, K. Mesenchymal stem cells engineered for cancer therapy. Adv. Drug Deliv. Rev. 2012, 64, 739–748.
44. Qiao, L.; Xu, Z.; Zhao, T.; Zhao, Z.; Shi, M.; Zhao, R.C.; Ye, L.; Zhang, X. Suppression of tumorigenesis by human mesenchymal stem cells in a hepatoma model. Cell Res. 2008, 18, 500.
45. Long, X.; Matsumoto, R.; Yang, P.; Uemura, T. Effect of human mesenchymal stem cells on the growth of HepG2 and Hela cells. Cell Struct. Funct. 2013, 38, 109-121.
46. Yu, Y.; Lu, L.; Qian, X.; Chen, N.; Yao, A.; Pu, L.; Zhang, F.; Li, X.; Kong, L.; Sun, B. Antifibrotic effect of hepatocyte growth factor-expressing mesenchymal stem cells in small-for-size liver transplant rats. Stem Cells Dev. 2009, 19, 903–914.
47. Hu, C.; Zhao, L.; Duan, J.; Li, L. Strategies to improve the efficiency of mesenchymal stem cell transplantation for reversal of liver fibrosis. J. Cell. Mol. Med. 2019, 23, 1657–1670.
48. Faidah, M.; Noorwali, A.; Atta, H.; Ahmed, N.; Habib, H.; Damiati, L.; Filimban, N.; Al-qriqri, M.; Mahfouz, S.; Khabaz, M.N. Mesenchymal stem cell therapy of hepatocellular carcinoma in rats: Detection of cell homing and tumor mass by magnetic resonance imaging using iron oxide nanoparticles. Adv. Clin. Exp. Med. 2017, 26, 1171–1178.
49. Lai, L.; Chen, J.; Wei, X.; Huang, M.; Hu, X.; Yang, R.; Jiang, X.; Shan, H. Transplantation of MSCs overexpressing HGF into a rat model of liver fibrosis. Mol. Imaging Biol. 2016, 18, 43–51.
50. Guimaraes, A.R.; Siqueira, L.; Uppal, R.; Alford, J.; Fuchs, B.C.; Yamada, S.; Tanabe, K.; Chung, R.T.; Lauwers, G.; Chew, M.L. T2 relaxation time is related to liver fibrosis severity. Quant. Imaging Med. Surg. 2016, 6, 103.
51. Wu, W.; Wu, Z.; Yu, T.; Jiang, C.; Kim, W.-S. Recent progress on magnetic iron oxide nanoparticles: Synthesis, surface functional strategies and biomedical applications. Sci. Technol. Adv. Mater. 2015, 16, 023501.
52. Li, Y.; Shang, W.; Liang, X.; Zeng, C.; Liu, M.; Wang, S.; Li, H.; Tian, J. The diagnosis of hepatic fibrosis by magnetic resonance and near-infrared imaging using dual-modality nanoparticles. RSC Adv. 2018, 8, 6699–6708.
53. Zhang, C.; Liu, H.; Cui, Y.; Li, X.; Zhang, Z.; Zhang, Y.; Wang, D. Molecular magnetic resonance imaging of activated hepatic stellate cells with ultrasmall superparamagnetic iron oxide targeting

integrin αvβ3 for staging liver fibrosis in rat model. Int. J. Nanomed. 2016, 11, 1097.

54. Wei, Y.; Zhao, M.; Yang, F.; Mao, Y.; Xie, H.; Zhou, Q. Iron overload by superparamagnetic iron oxide nanoparticles is a high risk factor in cirrhosis by a systems toxicology assessment. Sci. Rep. 2016, 6, 29110.
55. Lunov, O.; Syrovets, T.; Büchele, B.; Jiang, X.; Röcker, C.; Tron, K.; Nienhaus, G.U.; Walther, P.; Mailänder, V.; Landfester, K. The effect of carboxydextran-coated superparamagnetic iron oxide nanoparticles on c-Jun N-terminal kinase-mediated apoptosis in human macrophages. Biomaterials 2010, 31, 5063–5071.
56. Kolosnjaj-Tabi, J.; Lartigue, L.; Javed, Y.; Luciani, N.; Pellegrino, T.; Wilhelm, C.; Alloyeau, D.; Gazeau, F. Biotransformations of magnetic nanoparticles in the body. Nano Today 2016, 11, 280–284.
57. Yu, M.; Huang, S.; Yu, K.J.; Clyne, A.M. Dextran and polymer polyethylene glycol (PEG) coating reduce both 5 and 30 nm iron oxide nanoparticle cytotoxicity in 2D and 3D cell culture. Int. J. Mol. Sci. 2012, 13, 5554–5570.
58. Efremova, M.V.; Naumenko, V.A.; Spasova, M.; Garanina, A.S.; Abakumov, M.A.; Blokhina, A.D.; Melnikov, P.A.; Prelovskaya, A.O.; Heidelmann, M.; Li, Z.A. Magnetite-Gold nanohybrids as ideal all-in-one platforms for theranostics. Sci. Rep. 2018, 8, 11295.
59. Nguyen, T.; Mammeri, F.; Ammar, S. Iron oxide and gold based magneto-plasmonic nanostructures for medical applications: A review. Nanomaterials 2018, 8, 149.
60. Martinez-Boubeta, C.; Simeonidis, K.; Serantes, D.; Conde-Leborán, I.; Kazakis, I.; Stefanou, G.; Peña, L.; Galceran, R.; Balcells, L.; Monty, C. Adjustable Hyperthermia Response of Self-Assembled Ferromagnetic Fe-MgO Core–Shell Nanoparticles by Tuning Dipole–Dipole Interactions. Adv. Funct. Mater. 2012, 22, 3737–3744.
61. Lavorato, G.; Lima, E., Jr.; Vasquez Mansilla, M.; Troiani, H.; Zysler, R.; Winkler, E. Bifunctional CoFe2O4/ZnO core/shell nanoparticles for magnetic fluid hyperthermia with controlled optical response. J. Phys. Chem. C 2018, 122, 3047–3057.
62. Baeza, A.; Guisasola, E.; Ruiz-Hernandez, E.; Vallet-Regí, M. Magnetically triggered multidrug release by hybrid mesoporous silica nanoparticles. Chem. Mater. 2012, 24, 517–524.
63. El-Boubbou, K. Magnetic iron oxide nanoparticles as drug carriers: Clinical relevance. Nanomedicine 2018, 13, 953–971.
64. Kolosnjaj-Tabi, J.; Wilhelm, C. Magnetic nanoparticles in cancer therapy: How can thermal approaches help? Future Med. 2017, 12, 573-575.
65. Omelyanchik, A.; Efremova, M.; Myslitskaya, N.; Zybin, A.; Carey, B.J.; Sickel, J.; Kohl, H.; Bratschitsch, R.; Abakumov, M.; Majouga, A. Magnetic and Optical Properties of Gold-Coated Iron

Oxide Nanoparticles. J. Nanosci. Nanotechnol. 2019, 19, 4987–4993.

66. Salvatore, A.; Montis, C.; Berti, D.; Baglioni, P. Multifunctional Magnetoliposomes for Sequential Controlled Release. ACS Nano 2016, 10, 7749–7760.
67. Illés, E.; Tombácz, E. The effect of humic acid adsorption on pH-dependent surface charging and aggregation of magnetite nanoparticles. J. Colloid Interface Sci. 2006, 295, 115–123.
68. Ungureanu, B.S.; Teodorescuv, C.-M.; Săftoiu, A. Magnetic Nanoparticles for Hepatocellular Carcinoma Diagnosis and Therapy. J. Gastrointest. Liver Dis. 2016, 25.
69. Ferrucci, J.; Stark, D. Iron oxide-enhanced MR imaging of the liver and spleen: Review of the first 5 years. AJR. Am. J. Roentgenol. 1990, 155, 943–950.
70. Giavridis, T.; van der Stegen, S.J.C.; Eyquem, J.; Hamieh, M.; Piersigilli, A.; Sadelain, M. CAR T cell-induced cytokine release syndrome is mediated by macrophages and abated by IL-1 blockade. Nat. Med. 2018, 24, 731–738.
71. Rezvani, K.; Rouce, R.; Liu, E.; Shpall, E. Engineering Natural Killer Cells for Cancer Immunotherapy. Molecular therapy. J. Am. Soc. Gene Ther. 2017, 25, 1769–1781.
72. Kang, J.H.; Krause, S.; Tobin, H.; Mammoto, A.; Kanapathipillai, M.; Ingber, D.E. A combined micromagnetic-microfluidic device for rapid capture and culture of rare circulating tumor cells. Lab Chip 2012, 12, 2175–2181.
73. Liu, F.; KC, P.; Zhang, G.; Zhe, J. Microfluidic magnetic bead assay for cell detection. Anal. Chem. 2015, 88, 711–717.
74. Shields, C.W.; Reyes, C.D.; López, G.P. Microfluidic cell sorting: A review of the advances in the separation of cells from debulking to rare cell isolation. Lab Chip 2015, 15, 1230–1249.
75. Ito, A.; Takizawa, Y.; Honda, H.; Hata, K.-I.; Kagami, H.; Ueda, M.; Kobayashi, T. Tissue engineering using magnetite nanoparticles and magnetic force: Heterotypic layers of cocultured hepatocytes and endothelial cells. Tissue Eng. 2004, 10, 833–840.
76. Ito, A.; Hibino, E.; Kobayashi, C.; Terasaki, H.; Kagami, H.; Ueda, M.; Kobayashi, T.; Honda, H. Construction and delivery of tissue-engineered human retinal pigment epithelial cell sheets, using magnetite nanoparticles and magnetic force. Tissue Eng. 2005, 11, 489–496.
77. Omelyanchik, A.; Levada, E.; Ding, J.; Lendinez, S.; Pearson, J.; Efremova, M.; Bessalova, V.; Karpenkov, D.; Semenova, E.; Khlusov, I. Design of Conductive Microwire Systems for Manipulation of Biological Cells. IEEE Trans. Magn. 2018, 54, 1–5.
78. Okochi, M.; Matsumura, T.; Honda, H. Magnetic force-based cell patterning for evaluation of the effect of stromal fibroblasts on invasive capacity in 3Dcultures. Biosens. Bioelectron. 2013, 42, 300–307.

79. Okochi, M.; Matsumura, T.; Yamamoto, S.; Nakayama, E.; Jimbow, K.; Honda, H. Cell behavior observation and gene expression analysis of melanoma associated with stromal fibroblasts in a three-dimensional magnetic cell culture array. Biotechnol. Prog. 2013, 29, 135–142.
80. Tanase, M.; Felton, E.J.; Gray, D.S.; Hultgren, A.; Chen, C.S.; Reich, D.H. Assembly of multicellular constructs and microarrays of cells using magnetic nanowires. Lab Chip 2005, 5, 598–605.
81. Rieck, S.; Heun, Y.; Heidsieck, A.; Mykhaylyk, O.; Pfeifer, A.; Gleich, B.; Mannell, H.; Wenzel, D. Local anti-angiogenic therapy by magnet-assisted downregulation of SHP2 phosphatase. J. Controll. Release 2019, 305, 155–164.
82. Muthana, M.; Kennerley, A.J.; Hughes, R.; Fagnano, E.; Richardson, J.; Paul, M.; Murdoch, C.; Wright, F.; Payne, C.; Lythgoe, M.F.; et al. Directing cell therapy to anatomic target sites in vivo with magnetic resonance targeting. Nat. Commun. 2015, 6, 8009.
83. Wang, X.; Ho, C.; Tsatskis, Y.; Law, J.; Zhang, Z.; Zhu, M.; Dai, C.; Wang, F.; Tan, M.; Hopyan, S. Intracellular manipulation and measurement with multipole magnetic tweezers. Sci. Robot. 2019, 4, eaav6180.
84. Zamay, T.N.; Zamay, G.S.; Belyanina, I.V.; Zamay, S.S.; Denisenko, V.V.; Kolovskaya, O.S.; Ivanchenko, T.I.; Grigorieva, V.L.; Garanzha, I.V.; Veprintsev, D.V. Noninvasive Microsurgery Using Aptamer-Functionalized Magnetic Microdisks for Tumor Cell Eradication. Nucleic Acid Ther. 2017, 27, 105–114.
85. Golovin, Y.I.; Gribanovsky, S.L.; Golovin, D.Y.; Klyachko, N.L.; Majouga, A.G.; Master, A.M.; Sokolsky, M.; Kabanov, A.V. Towards nanomedicines of the future: Remote magneto-mechanical actuation of nanomedicines by alternating magnetic fields. J. Controll. Release 2015, 219, 43–60.
86. Du, V.; Luciani, N.; Richard, S.; Mary, G.; Gay, C.; Mazuel, F.; Reffay, M.; Menasche, P.; Agbulut, O.; Wilhelm, C. A 3D magnetic tissue stretcher for remote mechanical control of embryonic stem cell differentiation. Nat. Commun. 2017, 8, 400.
87. Sun, J.; Liu, X.; Huang, J.; Song, L.; Chen, Z.; Liu, H.; Li, Y.; Zhang, Y.; Gu, N. Magnetic assembly-mediated enhancement of differentiation of mouse bone marrow cells cultured on magnetic colloidal assemblies. Sci. Rep. 2014, 4, 5125.
88. Tseng, P.; Judy, J.W.; Di Carlo, D. Magnetic nanoparticle–mediated massively parallel mechanical modulation of single-cell behavior. Nat. Methods 2012, 9, 1113.
89. Kollmannsberger, P.; Fabry, B. BaHigh-force magnetic tweezers with force feedback for biological applications. Rev. Sci. Instrum. 2007, 78, 114301.
90. Lipfert, J.; Kerssemakers, J.W.; Jager, T.; Dekker, N.H. Magnetic torque tweezers: Measuring torsional stiffness in DNA and RecA-DNA filaments. Nat. Methods 2010, 7, 977.

91. Noh, S.-H.; Moon, S.H.; Shin, T.-H.; Lim, Y.; Cheon, J. Recent advances of magneto-thermal capabilities of nanoparticles: From design principles to biomedical applications. Nano Today 2017, 13, 61–76.
92. He, S.; Zhang, H.; Liu, Y.; Sun, F.; Yu, X.; Li, X.; Zhang, L.; Wang, L.; Mao, K.; Wang, G. Maximizing specific loss power for magnetic hyperthermia by hard–soft mixed ferrites. Small 2018, 14, 1800135.
93. Riedinger, A.; Guardia, P.; Curcio, A.; Garcia, M.A.; Cingolani, R.; Manna, L.; Pellegrino, T. Subnanometer local temperature probing and remotely controlled drug release based on azo-functionalized iron oxide nanoparticles. Nano Lett. 2013, 13, 2399–2406.
94. Fuller, E.G.; Sun, H.; Dhavalikar, R.D.; Unni, M.; Scheutz, G.M.; Sumerlin, B.S.; Rinaldi, C. Externally Triggered Heat and Drug Release from Magnetically Controlled Nanocarriers. ACS Appl. Polym. Mater. 2019, 1, 211–220.
95. Chen, W.; Cheng, C.-A.; Zink, J.I. Spatial, Temporal, and Dose Control of Drug Delivery using Noninvasive Magnetic Stimulation. ACS Nano 2019, 13, 1292–1308.
96. Tietze, R.; Zaloga, J.; Unterweger, H.; Lyer, S.; Friedrich, R.P.; Janko, C.; Pöttler, M.; Dürr, S.; Alexiou, C. Magnetic nanoparticle-based drug delivery for cancer therapy. Biochem. Biophys. Res. Commun. 2015, 468, 463–470.
97. Stimphil, E.; Nagesetti, A.; Guduru, R.; Stewart, T.; Rodzinski, A.; Liang, P.; Khizroev, S. Physics considerations in targeted anticancer drug delivery by magnetoelectric nanoparticles. Appl. Phys. Rev. 2017, 4, 021101.
98. Mulens, V.; Morales, M.d.P.; Barber, D.F. Development of magnetic nanoparticles for cancer gene therapy: A comprehensive review. ISRN Nanomat. 2013, 2013, 646284.
99. Scialabba, C.; Puleio, R.; Peddis, D.; Varvaro, G.; Calandra, P.; Cassata, G.; Cicero, L.; Licciardi, M.; Giammona, G. Folate targeted coated SPIONs as efficient tool for MRI. Nano Res. 2017, 10, 3212–3227.
100. Nielsen, M.J.; Veidal, S.S.; Karsdal, M.A.; Orsnes-Leeming, D.J.; Vainer, B.; Gardner, S.D.; Hamatake, R.; Goodman, Z.D.; Schuppan, D.; Patel, K. Plasma Pro-C3 (N-terminal type III collagen propeptide) predicts fibrosis progression in patients with chronic hepatitis C. Liver Int. 2015, 35, 429–437.
101. Bauer, L.M.; Situ, S.F.; Griswold, M.A.; Samia, A.C.S. Magnetic particle imaging tracers: State-of-the-art and future directions. J. Phys. Chem. Lett. 2015, 6, 2509–2517.
102. Nikitin, M.P.; Orlov, A.; Sokolov, I.; Minakov, A.; Nikitin, P.; Ding, J.; Bader, S.; Rozhkova, E.; Novosad, V. Ultrasensitive detection enabled by nonlinear magnetization of nanomagnetic labels. Nanoscale 2018, 10, 11642–11650.

103. Haun, J.B.; Yoon, T.J.; Lee, H.; Weissleder, R. Magnetic nanoparticle biosensors. Wiley Interdiscip. Rev. Nanomed. Nanobiotechnol. 2010, 2, 291–304.

104. Ehling, J.; Bartneck, M.; Fech, V.; Butzbach, B.; Cesati, R.; Botnar, R.; Lammers, T.; Tacke, F. Elastin-based molecular MRI of liver fibrosis. Hepatology 2013, 58, 1517–1518.

105. Nagórniewicz, B.; Mardhian, D.F.; Booijink, R.; Storm, G.; Prakash, J.; Bansal, R. Engineered Relaxin as theranostic nanomedicine to diagnose and ameliorate liver cirrhosis. Nanomedicine 2019, 17, 106–118.

106. Mardhian, D.F.; Storm, G.; Bansal, R.; Prakash, J. Nano-targeted relaxin impairs fibrosis and tumor growth in pancreatic cancer and improves the efficacy of gemcitabine in vivo. J. Controll. Release 2018, 290, 1–10.